

# Geological setting of Late Triassic porphyry Cu-Au mineralization at the Dillard Creek property near Merritt, southern British Columbia

Mitchell G. Mihalynuk<sup>1,a</sup> and James M. Logan<sup>1</sup>

<sup>1</sup> British Columbia Geological Survey, Ministry of Energy, Mines and Natural Gas, Victoria, BC, V8W 9N3

<sup>a</sup> corresponding author: Mitch.Mihalynuk@gov.bc.ca

Recommended citation: Mihalynuk, Mitchell G. and Logan, James M., 2013. Geological setting of Late Triassic porphyry Cu-Au mineralization at the Dillard Creek property near Merritt, southern British Columbia. In: Geological Fieldwork 2012, British Columbia Ministry of Energy, Mines and Natural Gas, British Columbia Geological Survey Paper 2013-1, pp. 97-113.

---

## Abstract

Porphyry copper mineralization in dioritic intrusive rocks that cut a volcanosedimentary section of the Nicola Group (Late Triassic) is exposed on the rolling hillsides and logging clearcuts at the Dillard Creek property, ~45 km southeast of Merritt. Three high-level tabular dioritic bodies display both potassic and calcic alteration assemblages. Two of the bodies (at the Primer South and Dill Lake prospects) are on the opposite limbs of a gently north-plunging syncline, and are partly elongated east-west. Although these bodies appear to form centres from which sets of moderately to steeply dipping diorite to quartz monzodiorite dikes (1 - >10 m wide) cut across the syncline, it remains unclear if they represent discrete stocks or sites of particularly high dike concentration. Geochemical and petrographic similarities between a hornblende-pyroxene volcanic breccia unit in the upper, predominantly epiclastic, part of the Nicola Group and the mineralized intrusions suggest emplacement of the latter shortly after a transition from mainly volcanic deposition, characterized by pyroxene (augite) units, to mainly epiclastic sedimentation. The apparent change in magma composition may signal increases in volatile and potassium content of the source region, chemical changes that enhance the Cu-Au fertility of the magma. Copper sulphides have commonly been liberated from the volcano-magmatic pile during low-grade metamorphism, demonstrating the high potential for Cu concentration by an efficient hydromagmatic system.

**Keywords:** Dillard Creek property, Dill Lake, Primer, copper gold porphyry, Nicola Group, Late Triassic, Quesnel terrane, potassic alteration, calcic alteration, litho geochemistry, Osprey Lake batholith, Pennask batholith, Kingsvale Group

---

## 1. Introduction

Field investigations in the Dillard Creek area between Merritt and Princeton (Fig. 1) in 2012, are part of the ongoing, province-wide porphyry copper project (Logan and Mihalynuk, 2005a). Project objectives include defining the geological setting and determining the structural and stratigraphic controls on porphyry Cu-Au ±Ag-Mo mineralization in Late Triassic and Early Jurassic arc rocks as an aid to mineral resource evaluation and exploration in the province. We report herein on fieldwork, petrography, and geochemistry of bedrock that underlies developed prospects near the headwaters of Dillard Creek (Fig. 2). In a companion paper (Mihalynuk and Logan, this volume), we provide a similar treatment for mineralization at Miner Mountain on the outskirts of Princeton, about 30 km south of Dillard Creek (see also Logan and Mihalynuk, 2013a, this volume).

## 2. Geological setting

Striking alignment of porphyry copper deposits along the magmatic axes of two arc terranes, Quesnel and Stikine (Coney et al., 1980) creates well-defined exploration targets in British Columbia. These arcs have the same Devonian through Triassic histories, including a remarkable metallogenic event: a pulse of metal-laden magmatism near the end of the Late Triassic, creating a

rich endowment of porphyry Cu-Au ±Ag-Pt-Pd deposits (Mihalynuk, 2010; Logan and Mihalynuk, 2013b). Tectonic events giving rise to this mineralizing pulse are discussed by Mihalynuk and Logan (this volume) and detailed in (Logan and Mihalynuk, 2013b). Herein we focus on the structural and stratigraphic setting of mineralization at the Dill Lake, Primer South, and Primer North developed prospects (Fig. 3; MINFILE 092HNE191, 55, 56). These prospects, at the headwaters of Dillard Creek, have collectively been referred to as the Dillard Creek property (Pringle, 1969). Late Triassic Nicola Group volcanosedimentary rocks that contain mineralization at the Dillard Creek property are interpreted to span the Late Triassic porphyry-forming event, based on correlation with layered and intrusive rocks to the west (Preto, 1979; Monger, 1989).

Younger rocks also occur in the map area (Fig. 3): granite of the Middle Jurassic Osprey Lake batholith intrude Nicola Group strata, and both are overlain by felsic volcanic rocks of the Cretaceous Spences Bridge Group (Monger, 1989; Massey et al., 2005).

## 3. Access and previous work

The Dillard Property can be reached by Highway 3 to Princeton, about 280 km east of Vancouver, then by following the Princeton-Summerland Road (8.5 km

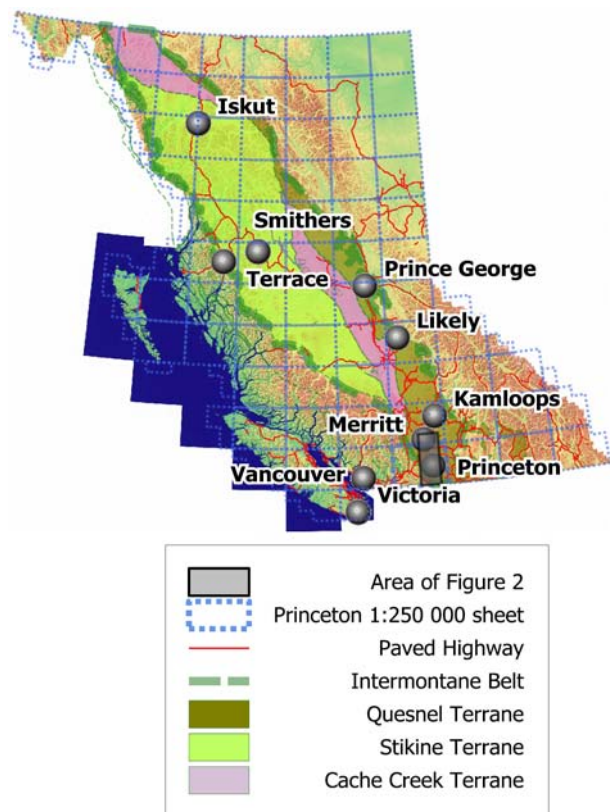


**Fig. 1.** Tectonic setting of southern Quesnel terrane and study area. Terrane boundaries modified after Tipper et al. (1981). Area of Figure 2 is shown by transparent grey box.

northeast) to the gravel Hembrie Mountain road and forest service roads (28 km north). Alternative access is via Highway 5 to Merritt, 260 km northeast of Vancouver, and then Highway 5A for 38 km southeast to the Loon Lake Road and gravel forest service roads that continue 20 km south to Dillard Lake. Most of the area is rolling and forested or clearcut (Fig. 4), with local steep rocky bluffs along glacial meltwater channels or modern valley sides.

Published maps covering the Dillard Property area at a scale appropriate for mineral exploration are lacking. Systematic regional mapping in the area dates to that of Rice (1947) and Monger (1989). The latter 1:250 000-scale map shows that the area is underlain by undivided “Eastern volcanic facies” mafic pyroclastic rocks and flows of the Nicola Group. Preto (1979) similarly defined the “Eastern Belt” west and northwest of the Dillard Property as submarine volcanic sedimentary rocks, lahar and basalt flows with comagmatic stocks. Mineral exploration in the area has resulted in a series of property-scale maps (e.g., Chapman, 1970; Guttrath, 1980) and drill hole logs (Tully, 1970).

#### 4. Dillard Creek area geology

Field observations in 2012 reveal a north-trending syncline in which various stratigraphic levels of the Late Triassic Nicola Group section are exposed, much like the Miner Mountain area to the south (Mihalynuk and Logan, this volume) and perhaps related to broad folds east of

Missezula Lake as recognized by Preto (1979). Layered rocks are cut by small dioritic intrusive “stocks” having irregular outlines, and associated with significant copper-gold mineralization, although, in the case of the Primer South and Dill Lake prospects, these “stocks” are, at least in part, concentrations of porphyritic dikes. Younger intrusions include the western edge of the Middle Jurassic Osprey Lake batholith and an isolated piece of the Early Jurassic Pennask batholith. The youngest rocks are previously unmapped exposures of rhyolite correlated with the Cretaceous Spences Bridge Group mapped ~3 km to the south (Massey et al., 2005). Alternatively, these rocks could belong to the Eocene Princeton Group. A sample has been collected for isotopic age determination.

Figure 3 draws upon the results of our reconnaissance mapping, and compiles mapping (Chapman, 1970; Guttrath, 1980) and drill core logging (Tully, 1970) from assessment reports. In cases where rock types logged at the top of the holes disagree with early mapping, we incorporate the drill hole data. This is particularly an issue in the Primer North area where rocks were previously mapped as undifferentiated Nicola Group andesites, but were logged as “feldspar porphyry”, in agreement with our field observations. Major improvements in access and number of outcrops exposed from road construction during recent logging aided our mapping.

On Figure 3, dikes are shown to extend for up to 2.5 km. The width of individual dikes is exaggerated; as portrayed, the dikes represent sets having the same orientation, with individual dikes 1 - >10 m thick. The composite tabular nature of the intrusions can be seen in the drill logs from Tully (1970). Some inclined drill holes at Primer South cut more than 300 m of nearly continuous intrusion.

#### 4.1. Layered rocks

Below we describe volcanic and sedimentary rocks in order of inferred ages, from oldest to youngest. We are unaware of any fossil or isotopic age data from rocks in this area, although the Nicola Group strata clearly extend beyond the map area to where their age is better defined.

##### 4.1.1. Coarse augite porphyry breccia

Crowded, coarse augite porphyries, the hallmark unit of the Nicola Group, are widespread in the study area. The porphyries constitute clasts in volcanic breccias and lesser lapilli tuffs, but are also in rare autobrecciated flows up to several metres thick. This unit is basaltic in composition, with SiO<sub>2</sub> contents of less than 52% (Table 1, e.g., 12JLO-5-54). Both fresh and weathered outcrops are typically green because of ubiquitous chlorite and epidote alteration (Fig. 5). However, surfaces where the weathered rind has not been removed by erosion can take on a tan, light grey, or even cream colouration. Outcrops are typically angular and blocky, but may appear pockmarked and hackly where thermally altered, due to clots of resistant secondary minerals. Euhedral black or dark green pyroxene can comprise up to 25% of the rock, and is accompanied by subequal amounts of plagioclase,

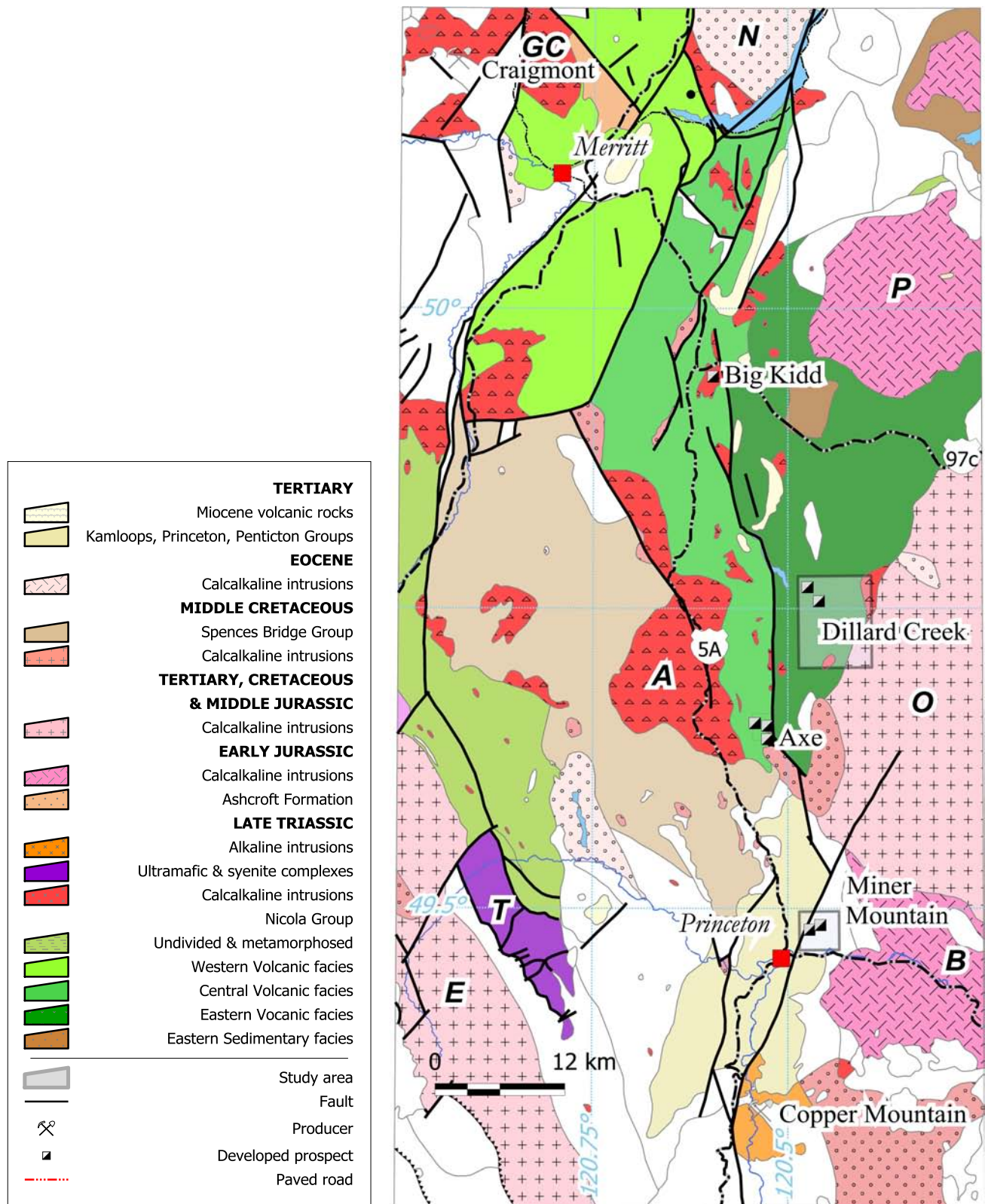


**Fig. 2.** Geological setting of 2012 field mapping in the Dillard Creek area between Princeton and Merritt (also shown is the Miner Mountain area; see Mihalynuk and Logan, this volume). Extents of Preto's Eastern Belt (mafic submarine volcanic and sedimentary rocks), Central Belt (arc axis, mafic volcanic and coeval intrusive rocks) and Western Belt (intermediate to felsic volcanic and sedimentary rocks) are shown for reference, as adapted from Massey et al. (2005). Abbreviations denote major plutons: A = Allison Lake, B = Bromley, E = Eagle, GC = Guichon Creek, N = Nicola, O = Osprey Lake, P = Pennask, T = Tulameen.

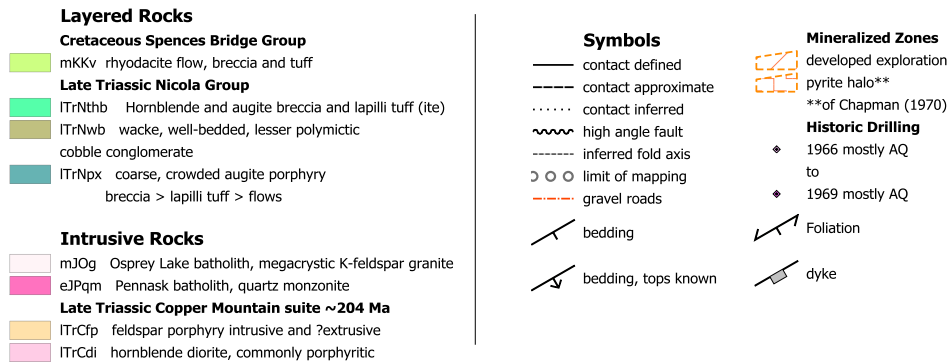
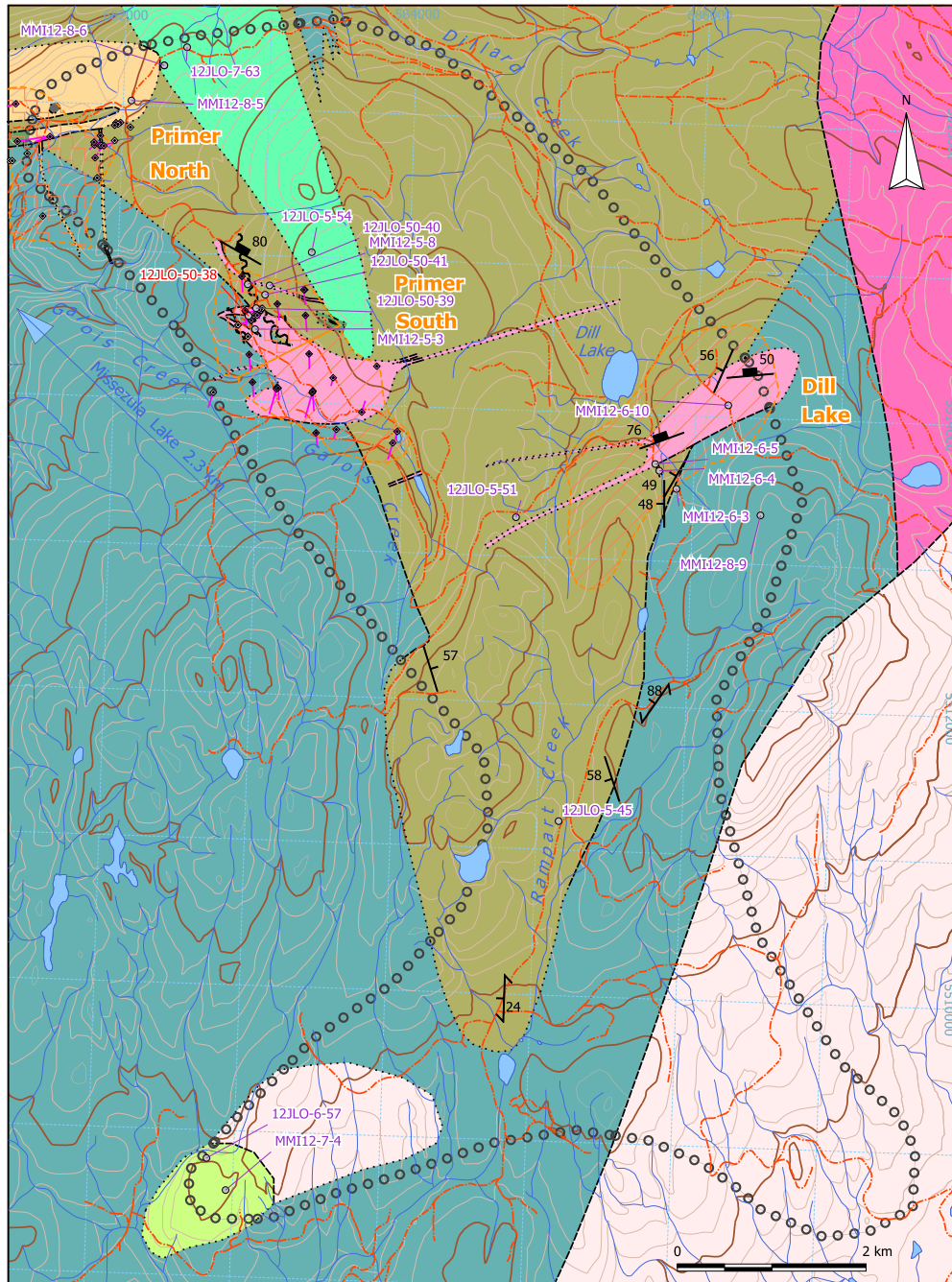


**Fig. 3.** Preliminary geology of the Dillard group of properties (Primer North, Primer South, Dill Lake); includes information compiled from Chapman (1970) and Gutrath (1980) and drill core logs from Tully (1970). Continuity and width of dikes may be exaggerated. Contacts with the Osprey Lake and Pennask batholiths are modified from Monger (1989).



**Fig. 4.** View from the eastern Dill property towards the west. Dill Lake (DL) is hidden in foreground valley on the right, with the Primer South property in the mid distance (PS, with patchy relics of forest).

which is altered to calcite, white mica, and prehnite, and 10% fine-grained magnetite that may be altered to hematite. Chlorite, calcite, and epidote veins are common.

#### 4.1.2. Hornblende-pyroxene porphyry

A layer of hornblende-rich pyroxene breccia interrupts the epiclastic succession above the main pyroxene-porphyry unit. It is of unknown extent, but is assumed to wedge out laterally into epiclastic strata to the south. Its northern extent is entirely unconstrained by our mapping. Coarse euhedral pyroxene and euhedral to anhedral hornblende occur in subequal abundances of 15-20% each. Hornblende is commonly embayed to sieve-textured, apparently in disequilibrium with the melt in which it travelled prior to solidifying. Both matrix and clasts appear to be of the same composition, thus we interpret the bed as a pyroclastic deposit, although an epiclastic mass flow origin cannot be ruled out.

#### 4.1.3. Epiclastic unit

An abrupt upward change from mainly pyroclastic to mainly epiclastic rocks is displayed in outcrops along the main haul road south of Dill Lake. The epiclastic rocks display prominent planar bedding (Fig. 7a), water escape structures, local synsedimentary slumps, and rare possible bioturbation structures. A lower unit, probably derived directly from underlying porphyries, comprises predominantly monomictic conglomerate to fine sandstone containing comminuted augite-phyric basalt fragments (Fig. 7a). An upper polymictic conglomerate unit contains augite-porphyry clasts and in similar proportions clasts also derived from the arc: hornblende and feldspar porphyries; hypabyssal intrusive rocks (diortite and monzonite); and sedimentary intraclasts (Fig. 7b). Our map coverage was insufficient to show subdivision of the epiclastic unit with any confidence.

#### 4.1.4. Rhyolite breccia (Spences Bridge Group?)

Previously unmapped, mauve, pink, and tan flow-banded rhyolite breccia forms low outcrops scattered over more than 1 km<sup>2</sup> of a new logging clearcut in the southern

part of the area (Fig. 3). Breccia clasts contain fine- to medium-grained oxyhornblende ±biotite (3%), rectangular sections of beta-quartz (1%), and plagioclase ±sanidine (up to 15% combined) phenocrysts in an aphanitic to very finely granular groundmass (devitrified glass?) (Fig. 8). In unaltered outcrops the feldspars appear fresh, but mafic minerals are rimmed by clay alteration. Chalcedonic quartz lines flattened vesicles that are typically less than 5 mm across.

The rhyolite is locally pyritic, and oxidation of pyrite has produced a strong acid alteration and bleaching. Where the pyritic rock is exposed in road cuts it is highly weathered, and stained red (hematite) or yellow (jarosite?). Very low magnetic susceptibilities seem typical. Geochemical analysis of a single grab sample returned negligible base and precious metal values, but elevated As values of 158 ppm (Table 2, 12JLO6-57). Another small outlier of young intermediate to felsic volcanic rocks is in the northwest corner of the map area. There, brown, scaly-weathering, highly vesicular volcanic rocks likely form a thin veneer atop altered porphyry.

The rhyolite unit is interpreted as a series of coalescing flow domes. We include these occurrences in the Spences Bridge Group to maintain a nomenclature consistent with the nearest post-Jurassic felsic volcanic package. However, some volcanic units within the Eocene Princeton Group are also rhyolite (Church, 1973). We collected a sample for isotopic age determination in order to resolve the uncertainty (MMI12-7-4; Fig. 3).

#### 4.2. Intrusive rocks

Intrusive rocks in the map area are correlated with suites of rocks that range from Late Triassic to Middle Jurassic. Of the intrusive rocks in the Dillard Lake area, only those correlated with the Middle Jurassic Osprey Lake batholith are demonstrably continuous with a well-dated body (166 ±1 Ma; Parrish and Monger, 1992). A wedge-shaped area in the northeast corner of the map area is underlain by intrusive rocks that are interpreted as an isolated part of the Early Jurassic Pennask batholith

**Table 1.** Major oxide analyses from Inductively Coupled Plasma – Mass Spectroscopy following lithium metaborate fusion of sample. Analyses performed at Activation Laboratories, Lancaster, Ontario. All values reported are weight %. Coordinates are UTM zone 10, North America Datum 1983.

StatNum	Unit	UTME	UTMN	SiO <sub>2</sub>	Al <sub>2</sub> O <sub>3</sub>	Fe <sub>2</sub> O <sub>3(T)</sub>	MnO	MgO	CaO	Na <sub>2</sub> O	K <sub>2</sub> O	TiO <sub>2</sub>	P <sub>2</sub> O <sub>5</sub>	LOI	Total
12JLO-5-54	ITrNpx	683327	5515033	48.33	15.81	10.51	0.257	4.93	7.98	3.04	3.65	0.743	0.57	3.93	99.74
12JLO-7-63	ITrNpx	682425	5516407	52.09	16.22	8.14	0.167	4.63	8.15	2.13	3.81	0.733	0.33	3.34	99.74
MM112-5-3	iTrCdi	682956	5514493	58.57	17.02	5.72	0.032	4.16	2.43	3.35	2.45	0.628	0.33	5.26	99.95
MM112-5-8	iTrCdi	683045	5514796	55.43	16.51	7.31	0.101	3.74	6.22	3.75	2.93	0.639	0.31	2.48	99.42
MM112-7-4	mKkv	682953	5508591	72.89	14.66	1.32	0.016	0.46	2.6	4.14	2.9	0.431	0.15	1.37	100.9
MM112-8-5	ITrCfp	682055	5516029	50.86	16.38	8.67	0.172	5.99	7.51	3.55	1.92	0.666	0.31	4.77	100.8
MM112-8-6	ITrNthb	682272	5516277	50.48	17.29	9.45	0.176	4.95	8.78	2.12	3.41	0.731	0.34	2.75	100.5
MM112-8-6b	ITrNthb	682272	5516277	50.2	17.15	9.42	0.175	4.92	8.84	2.1	3.37	0.728	0.36	2.76	100
MM112-8-9	ITrNpx	686467	5513337	49.24	13.34	10.92	0.221	8.11	11.91	2.42	1.43	1.104	0.29	1.34	100.3
Std MRG-1				38.59	8.43	17.42	0.167	13.26	14.72	0.71	0.18	3.705	0.07	1.45	98.71
Std WGB-1				48.83	10.91	6.33	0.135	9.14	16.34	2.15	0.91	0.885	0.09	3.8	99.51
			Det.				0.001	0.01							
			Limit	0.01%	0.01%	0.01%	%	%	0.01%	0.01%	0.01%	0.001%	0.01%	%	0.01%



**Fig. 5.** Typical augite-phyric volcanic breccia of the Nicola Group. Augite crystals are more obvious on some strongly weathered surfaces (Fig. 6).

(Massey et al., 2005), which has a U-Pb zircon age of ~195 Ma (Logan et al., 2011). Ages of other intrusive rocks are inferred on the basis of association and relative geological relationships.

#### 4.2.1. Copper Mountain suite hornblende diorite

Hornblende diorite (to quartz monzodiorite) intrusions that cut Nicola Group strata have been the focus of mineral exploration in the Dillard Creek area. In part, these intrusions consist of a series of easterly trending dikes, some of which extend for up to 2.5 km (if intermittently exposed sections of dike along trend belong to the same body). The dikes are typically moderately to steeply dipping (both north and south), and may be 1 m to more than 10 m wide. Depicted schematically in Figure 3, are the two southern mineralized intrusions at Primer South and Dill Lake, which seem to be areas where hornblende diorite dikes are concentrated. The intrusion at Primer North is a hornblende-feldspar porphyry of a different character (see below).

Where unaltered, the hornblende diorite forms blocky light to dark grey outcrops. It is medium- to coarse-grained, with black hornblende (10-20%) and vitreous, zoned feldspar (70-80%). Isolated hornblende and feldspar crystals are up to 2 cm long. Fine, irregular, commonly embayed grains of magnetite comprise ~3% of the rock. Some variants are quartz monzodiorite. For example, where orthoclase is more abundant than

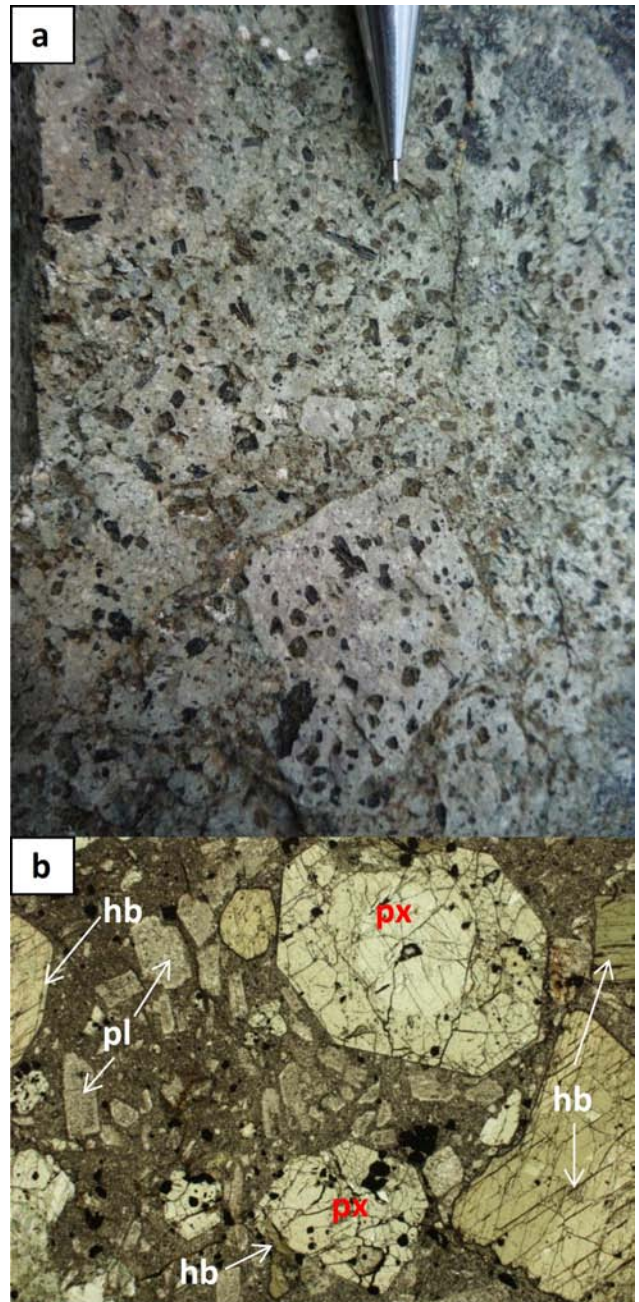


**Fig. 6.** Coarse zoned pyroxene and hornblende-phyric breccia in outcrop **a**) and in thin section **b**). In **b**), hb = hornblende and px = zoned pyroxene; note pyroxene at bottom centre partly engulfs a hornblende crystal. Turbid plagioclase is medium grained in a devitrified matrix with fine granular opaque minerals. Field of view is 4 mm.

plagioclase, and where the little matrix that exists in the holocrystalline intrusions is quartz, it comprises as much as 10% of the rock. Porphyritic intrusions can be crowded or sparsely populated with 1-10 mm subhedral hornblende laths and 2-5 mm plagioclase (and sanidine?) in a devitrified groundmass dusted with magnetite. A trachytic alignment of the crystals is common in both holocrystalline and porphyritic variants. Where mineralized, chalcopyrite is disseminated, and most broken samples contain a paper thin chalcopyrite veinlet

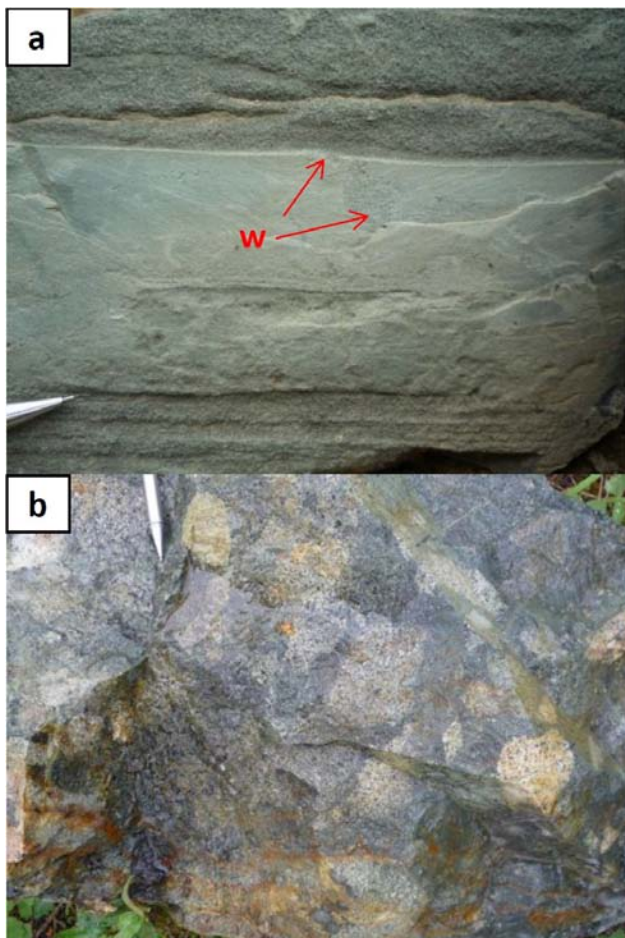


**Fig. 7.** Epiclastic unit. **a)** Well-bedded sandstones derived from augite-porphry volcanic units (W = possible bioturbation or water escape features). **b)** Coarse polymictic conglomerate containing clasts of hypabyssal hornblende-feldspar porphyry-like units that cut the underlying augite porphyry breccia unit.

or two. Rounded xenoliths of pyroxene-phyric volcanic rock are common. Magnetic susceptibilities range between 20 and  $45 \times 10^{-5}$  SI (and higher or lower where altered).

At the Dill Lake prospect, coarse trachytic plagioclase- and hornblende-phyric monzodiorite intrudes thinly bedded and bleached, pyritic (1-2%) sandstone. The monzodiorite is white weathering and massive to well jointed. Euhedral, white stubby plagioclase phenocrysts are 3-5 mm in size. Hornblende is 2-3 mm long and, together with the intrusive groundmass, is altered to epidote, actinolite, chlorite, quartz and pyrite (~1%) (Fig. 9). Disseminated magnetite is common and magnetic susceptibilities range between 17 and  $35 \times 10^{-5}$  SI.

On the west side of Primer South is an area of a few 100 m<sup>2</sup> with sparse outcrops of medium- to coarse-grained pyroxene-hornblende gabbro with 50% coarse plagioclase and hornblende (after pyroxene?) in a fine-grained, white, feldspathic groundmass. Gossanous “veins” up to 15 cm thick contain traces of malachite and



**Fig. 8.** Rhyolite breccia clasts containing oxyhornblende (±biotite)-quartz-plagioclase ±sanidine-porphyrific rhyolite. This unit is mapped as the mid-Cretaceous Spences Bridge Group, but could be part of the Eocene Princeton Group.

are probably weathered-out pyrite with minor chalcopyrite. This gabbro is interpreted as a border phase, intrusive-country rock hybrid. Magnetic susceptibilities are near  $100 \times 10^{-5}$  SI.

Like other workers (e.g., Preto, 1979; Monger, 1989; and authors of most assessment reports cited herein) we assume these intrusions equivalent with the Late Triassic Copper Mountain suite. We collected a sample with fresh hornblende for <sup>40</sup>Ar/<sup>39</sup>Ar isotopic age determination (MMI12-5-8) to test this correlation. These intrusions cut both the augite porphyry units and the lower epiclastic package, but also appear to have provided detritus for polymictic conglomerates higher in the Nicola Group stratigraphy. On this basis, they should be Late Triassic in age, broadly time equivalent to mineralizing intrusions at Copper Mountain (Mihalynuk et al., 2010). If the mineralized intrusions at Dill Lake and Primer South did form as a dense concentration of dikes, this mode of occurrence is different than the discrete stocks at Copper Mountain. However, significant copper mineralization associated with dike concentrations is not unprecedented in British Columbia. One good example of an alkalic porphyry Cu-Au deposit where the mineralizing intrusions are dike-like, is the massive Galore Creek deposit in northwestern part of the province.

**Table 2.** Base metal and Pt, Pd analytical values from samples collected in the Dillard Creek area, away from localities obviously sampled previously. Analyses performed by Inductively Coupled Plasma – Mass Spectroscopy (ICP-MS) at Acme Analytical Laboratories Ltd., Vancouver. For a full suite of elements analyzed see Mihalynuk and Logan (2013b). Coordinates are UTM zone 10, North America Datum 1983.

StatNum	UTME	UTMN	Mo	Cu	Pb	Zn	Ag	Ni	Fe	As	Au	Sb	Bi	V
12JLO-5-45	685153	5511196	0.15	125.55	3.13	27.3	121	4.8	2.48	1.9	1.4	0.1	0.22	83
12JLO-5-51	684790	5513267	77.38	29.34	1	10.6	308	4.9	2.97	3.1	4.9	0.15	0.17	94
12JLO-6-57	682815	5508807	14.64	41.84	0.88	18.8	25	4.2	1.22	158.3	<0.2	0.1	0.11	31
12JLO-8-81	677388	5503059	0.34	3689.06	1.2	57.7	648	7.3	3.12	4.8	337.5	0.32	<0.02	109
MM112-6-3	685884	5513498	0.48	333.28	3.09	69.9	1125	22.1	3.25	6.1	135.2	0.1	0.46	101
MM112-6-4	685762	5513618	0.32	350.86	4.84	71.3	223	14.2	3.02	2.8	7.2	0.27	0.05	145
MM112-6-5	685733	5513664	3.08	715.9	16.52	58.3	708	11.1	1.93	3.5	18.1	0.21	0.19	93
MM112-6-10	686220	5514083	0.05	29.44	1.35	10.5	99	11.1	2.38	1.9	73.9	0.14	0.18	91
MM112-6-10b	686220	5514083	0.13	281.28	1.86	14.7	431	11.6	2.33	2.7	67	0.29	0.32	79
12JLO50-30	685019	5484773	5.12	131.1	1.29	22.6	399	3.3	1.55	8.1	38.3	1.67	0.02	12
12JLO50-38-3	682908	5514583	0.03	4.09	2.12	65	17	3.1	3.23	0.6	1.8	0.1	<0.02	98
12JLO50-39	682958	5514637	4.79	111.04	0.77	25.7	68	5.2	2.13	1.6	1.1	0.13	<0.02	28
Std WGB-1			0.85	7204.1	11.27	79.4	3046	3418.4	7.98	3.8	181.1	0.86	0.29	59
Std BCGS till1999			0.85	202.65	236.64	352.5	1752	293.2	7.35	66.9	62	11.12	0.28	135
Std BCGS till1999			0.73	183.46	220.27	334.4	1660	214.2	7.34	61.9	27.1	7.86	0.22	103
STD DS9			15.24	111.43	140.49	345.5	1981	40.6	2.34	28.4	140	5.69	8.03	54
STD DS9			12.97	113.43	130.1	312.9	1793	41.3	2.38	27	108.8	5.25	5.94	41
			ppm	ppm	ppm	ppm	ppb	ppm	%	ppm	ppb	ppm	ppm	ppm
		det. Limit	0.01	0.01	0.01	0.1	2	0.1	0.01	0.1	0.2	0.02	0.02	2

Table 2. Continued.

StatNum	UTME	UTMN	Ca	P	La	Cr	Mg	Na	K	S	Hg	Se	Pd	Pt
12JLO-5-45	685153	5511196	0.88	0.086	6.6	59.1	0.68	0.092	0.38	<0.02	<5	<0.1	<10	<2
12JLO-5-51	684790	5513267	2.44	0.19	3.6	24.8	0.48	0.04	0.05	1.96	33	0.6	21	7
12JLO-6-57	682815	5508807	0.08	0.037	3.5	26.9	0.04	0.065	0.1	0.67	<5	<0.1	<10	<2
12JLO-8-81	677388	5503059	0.79	0.102	2.8	19.8	1.36	0.051	0.1	0.03	14	2.3	<10	<2
MM112-6-3	685884	5513498	0.82	0.136	3.5	40.5	1.48	0.064	1.04	0.69	9	0.8	<10	4
MM112-6-4	685762	5513618	0.98	0.134	1.8	48	1.54	0.093	0.46	0.04	24	0.2	<10	4
MM112-6-5	685733	5513664	0.89	0.141	7.4	34.2	0.98	0.06	0.11	0.07	29	0.5	<10	2
MM112-6-10	686220	5514083	1.15	0.119	1.9	52.6	0.43	0.168	0.41	2.01	250	0.9	<10	2
MM112-6-10b	686220	5514083	0.94	0.124	2.1	35.2	0.56	0.098	0.16	1.05	281	2.4	<10	4
12JLO50-30	685019	5484773	4.03	0.053	2.5	34.1	0.4	0.049	0.18	0.13	21	0.6	<10	<2
12JLO50-38-3	682908	5514583	1.74	0.116	20.3	43.3	1.17	0.149	1.58	0.04	16	0.2	<10	<2
12JLO50-39	682958	5514637	1.07	0.057	2.9	55	0.54	0.15	0.16	0.61	8	1.4	<10	<2
Std WGB-1			1.71	0.058	3.2	275.5	2.56	0.007	0.02	3.04	154	14.2	431	212
Std BCGS tii11999			0.36	0.119	14.4	265.8	2.74	0.004	0.05	<0.02	371	0.7	<10	<2
Std BCGS ti111999			0.35	0.114	13.4	236.7	2.84	0.01	0.05	<0.02	295	0.7	<10	<2
STD DS9			0.74	0.09	15.5	132.3	0.62	0.085	0.4	0.17	224	6	135	405
STD DS9			0.72	0.087	12.5	115.6	0.63	0.083	0.41	0.17	206	5.6	124	332
			%	%	ppm	ppm	%	%	%	%	ppb	ppm	ppb	ppb
		det. Limit	0.01	0.001	0.5	0.5	0.01	0.001	0.01	0.02	5	0.1	10	2



**Fig. 9.** Chlorite-epidote altered porphyritic diorite displays pale green epidote vein selvage alteration overprinted on a broader K-feldspar flush. Dark green-black vein in centre of photo is chlorite-actinolite-pyrite with minor chalcopyrite.

#### 4.2.2. Feldspar porphyry intrusives and flows?

Coarse hornblende- and medium-grained feldspar porphyry forms blocky outcrops at the Primer North prospect. A strong trachytic fabric is generally displayed. The rock may be relatively fresh, cut by widely spaced epidote and calcite veins, or pervasively pyritic  $\pm$ biotite-flooded and indurated. Where altered, granular feldspar comprises  $\sim$ 70% of the rock, together with 15% fine-grained secondary biotite (and chlorite) and up to 5% pyrite in clots and veins up to 5 mm thick. Alteration masks contacts between the porphyry and surrounding pyroxene-bearing tuffite. Even at fresh exposures, we were unable to unequivocally determine whether this unit represents flows or a hypabyssal intrusion. We correlate this unit with the Copper Mountain suite, following earlier interpretations, but careful mapping and geochronologic work are needed to verify this assumption.

#### 4.2.3. Monzonite dikes

At the Primer North property a series of orange to pink or white felsic dikes cut indurated, hornfelsed, pyritic epiclastic country rocks. They are steep, north-trending, 1.5 -  $>$ 3.5 m wide, and display sharp, chilled contacts. Medium-grained, salmon pink feldspar comprises  $\sim$ 40% of the rock within an altered white groundmass; where less altered, the feldspars are white in

a pink groundmass. In either case, mafic minerals are totally replaced by clots of chlorite.

#### 4.2.4. Osprey Lake granite

Osprey Lake batholith is a large composite intrusive complex that extends from the map area to ridges west of Okanagan Lake,  $\sim$ 70 km away. As expected for a body of this size, the country rocks display a strong thermal-metamorphic halo, which extends for at least 0.5 km from its western contact into the study area.

Typical outcrops of Osprey Lake granite are white to pinkish-grey and rounded to blocky. Conspicuous K-feldspar megacrysts up to 5 cm (20%) are supported by a groundmass of medium- to coarse-grained plagioclase, orthoclase, and grey quartz (Fig. 10). Megacrysts have zones outlined by hornblende microlytes and exterior zones that are white albite (?). Medium-grained biotite forms 3-5 mm euhedral to subhedral books. It constitutes  $\sim$ 10% of the rock, and medium-grained hornblende comprises  $\sim$ 6%. Equant plagioclase and pinkish matrix K-feldspar comprises  $\sim$ 60% of the rock volume. Accessory minerals identifiable in hand sample include euhedral, honey brown titanite (0.5-1%) and magnetite. Xenoliths of hornblende diorite are common. Magnetic susceptibilities range between 20 and  $38 \times 10^{-5}$  SI.

#### 4.2.5. Rhyolite dikes

Decimetre wide dikes of white to pale pink, quartz-eye porphyry rhyolite intrude hornblende diorite at the Primer South prospect. The rock is characteristically flow-banded, fine grained, and contains miarolitic cavities. Relict 1-2 mm biotite and oxidized pyrite crystals are visible in a pervasive quartz-sericite-pyrite- and clay-altered groundmass. Unlike intrusions of presumed Late Triassic age, malachite was not visible within or adjacent to the dike contacts. Magnetic susceptibility values are very low.

These felsic dikes are lithologically similar to the rhyolite flows identified in the southern part of the map area, and may represent feeders to the Cretaceous Spences Bridge Group.

### 5. Litho geochemistry

Representative samples were collected from the Dillard Creek area for major oxide and trace element analysis with a bias towards the mafic part of the Late Triassic stratigraphy: hornblende and pyroxene-phyric breccia units and diorite. Major oxide analyses are reported in Table 1; major and trace element analyses are available in downloadable format from Mihalynuk and Logan (2013b). Select major oxide and trace element concentrations are shown on Figure 11.

Most pyroxene porphyry samples, and all of the hornblende-pyroxene tuff samples, fall within the shoshonitic basalt series, based on the  $K_2O$  versus  $SiO_2$  classification of Peccerillo and Taylor (1976; Fig. 11a). Diorite samples belong to the high-K calcalkaline series, and their volcanic equivalents range from basalt (MMI12-8-5) to andesite (MMI12-5-3). The Spences Bridge

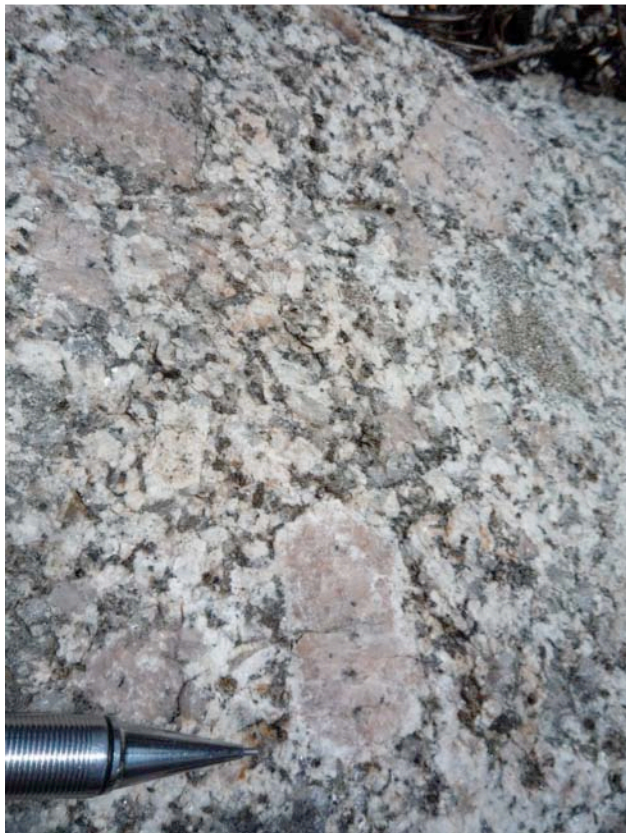


**Fig. 10.** Distinctive zoned K-feldspar megacrysts in Osprey Lake batholith.

rhyolite sample is shown by the star in Figures 11a and 11b.  $\text{Na}_2\text{O}$  contents of all mafic volcanic rocks exceed 2 weight % (represented by green bars on Fig. 11a), so that on the Total alkalis - silica space ( $\text{Na}_2\text{O} + \text{K}_2\text{O}$  vs.  $\text{SiO}_2$ , not shown) they are also classified as alkaline ( $>5\%$   $\text{Na}_2\text{O} + \text{K}_2\text{O}$ ) over the range of basalt to basaltic andesite (LeBas et al., 1986).

In contrast, application of the trace element alkalinity index Nb/Y (Pearce, 1996) shows that the mafic volcanic units are not alkaline (Fig. 11b). In some environments, this discrepancy could be attributed to addition of alkalis during alteration, an especially likely event in volcanic rocks deposited in a submarine environment, as has been interpreted regionally (e.g., Preto, 1979). In this case however, the low Nb/Y index arises from the deep Nb-Ta depletion: a strong arc signature, as shown on the Primitive Mantle – normalized spider diagram (Sun and McDonough, 1989) of Figure 11c. Samples collected from hornblende diorite intrusive units that cut the basalts, display the same range of Nb/Y as do samples of Nicola Group from elsewhere, including units known to contain analcime (Preto, 1979; shown as grey triangles with olive outlines on Fig. 11b). Thus, the intrusions are interpreted as comagmatic with the basalts, a contention supported by clasts of hornblende diorite within strata intercalated with the volcanic units.

Other geochemical features of arc basalt include Ti depletion and enrichment in large ion lithophile elements

shown on the left side of Figure 11c (e.g., Cs, Rb, Ba, K, Sr). These rocks lack a Eu anomaly (Figs. 11c, d), suggesting that feldspar was neither a residual phase in the source area, nor was it removed from the crystallizing melt. All units are uniformly light rare earth element (LREE) enriched compared to chondrite values (Fig. 13d; Sun and McDonough, 1989) and show similar parentage (Figs. 11c, d). However, a systematic increase in heavy rare earth elements in hornblende-bearing samples may indicate magmatic contributions from a region that sequesters HREE, perhaps garnet-bearing metasomatized mantle. Shaded fields on both Figures 11c and 11d are those of mafic volcanic and dioritic rocks in the Miner Mountain area. They are nearly identical in geochemical character to the rocks at Dillard Creek, but show a definite relative LREE enrichment.

## 6. Alteration and mineralization

Early mapping of alteration zones at the Dillard Creek property (Chapman, 1970), partly delimited zones of pyrite (Fig. 3). These zones are superimposed on regional prehnite-pumpellyite grade metamorphic mineral assemblages (prehnite and/or pumpellyite and epidote-chlorite-albite) that are typically developed in the augite porphyries and derived volcaniclastic rocks of the Nicola Group (Fig. 12). Our mapping was insufficiently detailed to permit delineation of authigenic mineral zones. However, different alteration assemblages are associated with different intrusive phases. Hornblende diorite (to quartz monzonite) at Dill Lake and Primer South display both calcic and potassic alteration assemblages including actinolite-epidote-magnetite-calcium carbonate-pyrite-chalcopyrite  $\pm$ quartz, and K-feldspar-biotite-magnetite-chalcopyrite  $\pm$ pyrite (with minor inclusions of pyrrhotite) (Fig. 13).

Calcic alteration assemblages are predominant near trenches at the Primer South and Dill Lake prospects. Potassic alteration is subordinate and apparently younger, although timing is not well established. Secondary biotite and chalcopyrite assemblages at Primer South are cut by quartz veinlets containing carbonate, sulphides, and (?) gold values (e.g., MMI12-6-3, Table 2). Gold is also associated with quartz carbonate veins cutting albite-actinolite-epidote-pyrite- altered hornblende diorite in the area around Dill Lake (Cormier, 1990; Table 2).

In addition, carbonate alteration of some dikes is intense (Fig. 12b) and includes calcite ( $\pm$ Mg and Fe carbonates?) - pyrite  $\pm$  white mica  $\pm$  quartz. At Primer South, carbonate alteration seems to be related to a specific suite of dikes, but nowhere did we see the same dikes pass from an intensely altered to unaltered state. And because all carbonate-altered dikes seem to contain relicts of both hornblende and plagioclase, they cannot be distinguished, on this basis, from the other mineralized diorite dikes.

## 7. Structure

Bedding orientations and the distribution of volcanic and sedimentary facies outline a broad syncline that plunges gently and opens to the north. Outcrops in the

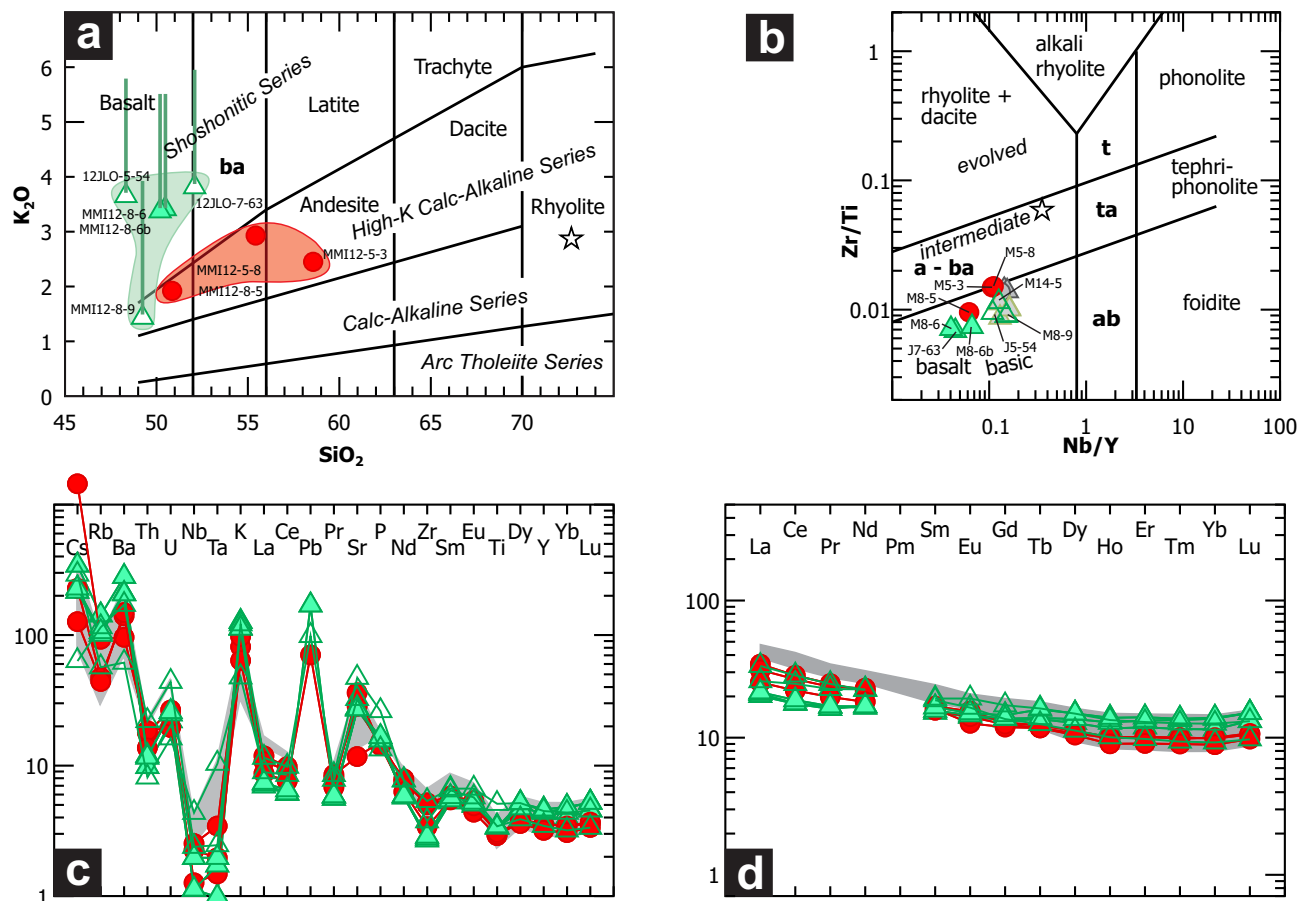


**Fig. 11.** Geochemical character of pyroxene-phyric basalt (open triangle), hornblende-pyroxene-phyric basalt (green-filled triangle), diorite (solid red circle, includes hornblende-feldspar porphyry of Primer North, MMI12-8-5), and Spences Bridge Group rhyolite (star), are shown by **a**) Plot of  $K_2O$  versus  $SiO_2$ , fields after (Peccerillo and Taylor, 1976), with oxides normalized with removal of components lost on ignition (LOI – see Table 1). **b**)  $Zr/Ti$  versus  $Nb/Y$  with fields after (Pearce, 1996). **c**) Primitive mantle normalized spider diagram and **d**) Chondrite-normalized rare earth element plot, using normalization factors of (Sun and McDonough, 1989). Abbreviations: a = andesite, ab = alkali basalt, ba = basaltic andesite, t = trachyte, ta = trachyandesite. Grey fields on c) and d) and dark grey-outlined grey symbols on b) are from similar rocks in the Miner Mountain area (Mihalynuk and Logan, this volume), olive-outlined grey symbols in b) are from analcime-bearing Nicola Group basalt (analcime identified by Preto, 1979).

hinge zone display a strong, near-vertical foliation indicating an upright fold. A shallow foliation near the southern limits of mapping is imparted by intrusion of the Osprey Lake batholith and partly defined by growth of garnet, epidote and hornblende.

Steeply dipping brittle fault zones are common, but the limited exposures do not provide opportunities to assess the amount or sense of offset. Slickenside orientations reveal no clear regional trends. If dikes can be traced for kilometres, as we infer on Figure 3, horizontal offsets on faults at high angles to the dikes must be minimal within the map area.

## 8. Summary

Dillard Creek property is located within the submarine volcanic and sedimentary “Eastern Belt” of (Preto, 1979). Mineralized intrusive centres at Dill Lake, Primer South and Primer North are all related to irregular

or east-west elongated hornblende feldspar porphyry or holocrystalline diorite to quartz monzodiorite bodies.

These bodies intrude both the east and west flanks of a gently north-plunging syncline. The Dill and Primer South bodies appear to have been centres from which moderately to steeply dipping dikes cut across the syncline. It is uncertain however, if the bodies are continuous “stocks” or sites of high dike concentration. Hypabyssal dioritic clasts within the sedimentary succession may indicate pencontemporaneous unroofing of the shallow (?) dioritic intrusions or erosion of their eruptive equivalents.

A transition from pyroxene to hornblende-pyroxene-phyric volcanic strata may mark an increase in the water and potassium content of the arc magma source. Presence of hornblende might indicate that the pyroxene-dominated arc magma was recharged from a more hydrated and potassium-rich source region or by a more evolved

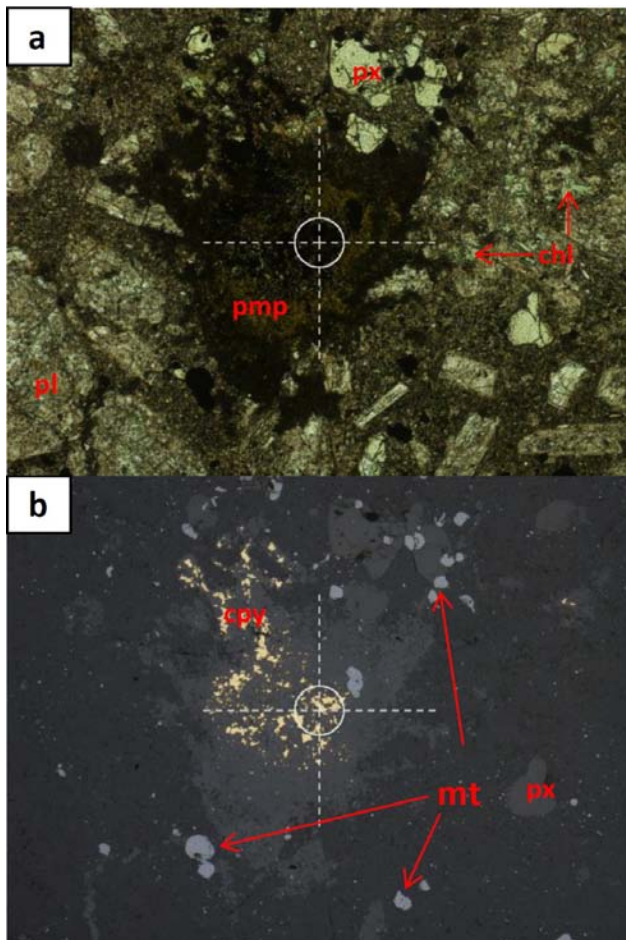


**Fig. 12.** **a)** Hornblende-pyroxene-feldspar porphyry with secondary chlorite (chl) and a patch of pumpellyite (pmp) with minor intergrown epidote at the centre of the photomicrograph. Plagioclase phenocrysts (pl) are made turbid by calcite and white mica alteration (in plane polarized light). In other samples, prehnite alters feldspars. **b)** The same field of view as in a) in reflected light shows chalcopyrite intergrowth with pumpellyite as an indication of the copper content of this rock, mobilized during low-grade metamorphism. Light grey rounded grains are magnetite; smooth dark grey crystals are pyroxene. Radius of the circle at crosshairs is 100 $\mu$ .

magma permitting growth or introduction of hornblende, followed by loss of volatiles and destabilization of hornblende. This same pyroxene to hornblende-bearing transition occurs at Miner Mountain (Mihalynuk and Logan, this volume) and other Late Triassic porphyry camps such as at the Iron Mask (Logan and Mihalynuk, 2005b) and Mount Polley (Logan and Mihalynuk, 2005c), and may be an important indicator of changing arc chemistry and fertility. Because of its potential importance to mineral exploration, we would like to establish whether or not this chemical change is coeval with the mineralizing epoch along the Late Triassic arc. Based on the appearance of hornblende-pyroxene-phyrlic volcanic strata in the predominantly epiclastic upper part of the Nicola Group, this chemical change may have occurred at about the same time as emplacement of the mineralized plutons at the Dillard Creek property. As a

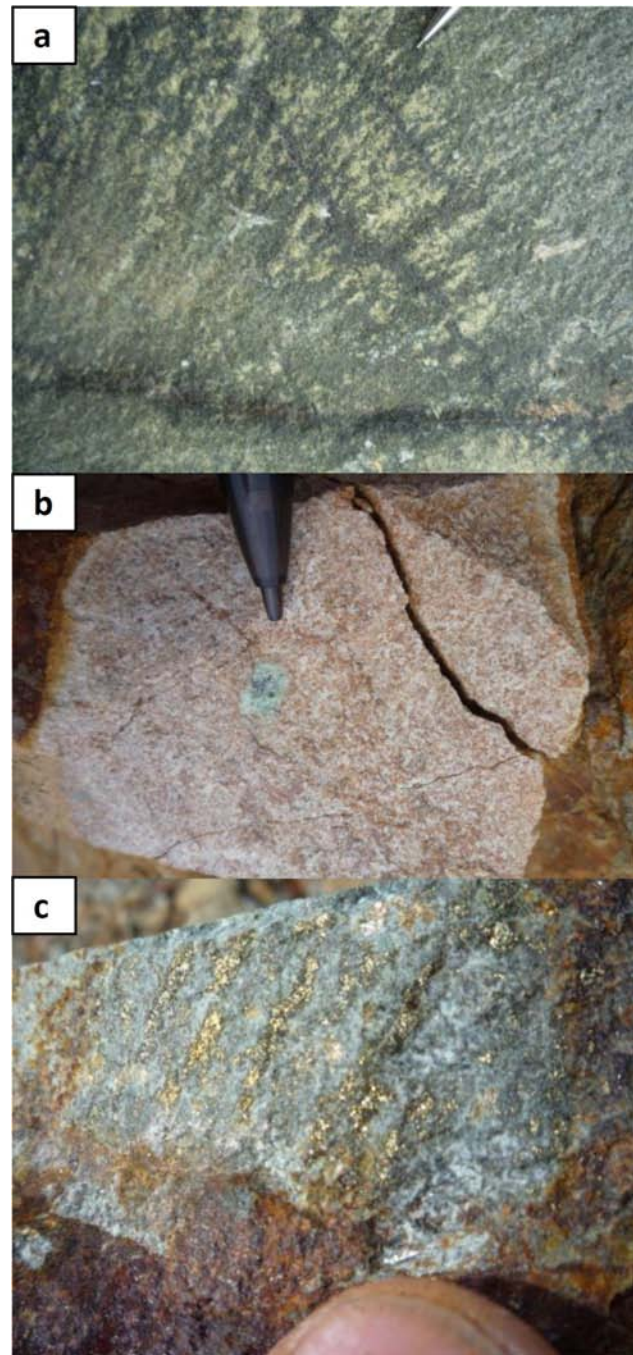


**Fig. 13.** Three styles of alteration and mineralization on the Dillard Creek property. **a)** Chlorite lined joints and thin veins  $\pm$  epidote and medial chalcopyrite. **b)** Strong carbonate alteration of trachytic? diorite. Parts of this same outcrop contain zones with secondary biotite alteration (see Fig. 14a). **c)** Within 50 m of the sample shown in Figure 14a, altered diorite is cut by secondary actinolite-magnetite-chalcopyrite veins (rusty material at bottom, see photomicrograph 14b, c). The irregular fracture surface obliquely intersects chalcopyrite and pyrite veinlets. A  $\sim 7\mu$  gold inclusion was found in an irregular crystal of pyrite from this locality (Fig. 15). Sample is from near the collars of DDH 1966-1 and DDH 1991-8 (Tully, 1970; Fig. 3).

preliminary test, we have collected samples for isotopic age determinations to establish if the two events are synchronous. Both pyroxene- and pyroxene-hornblende-

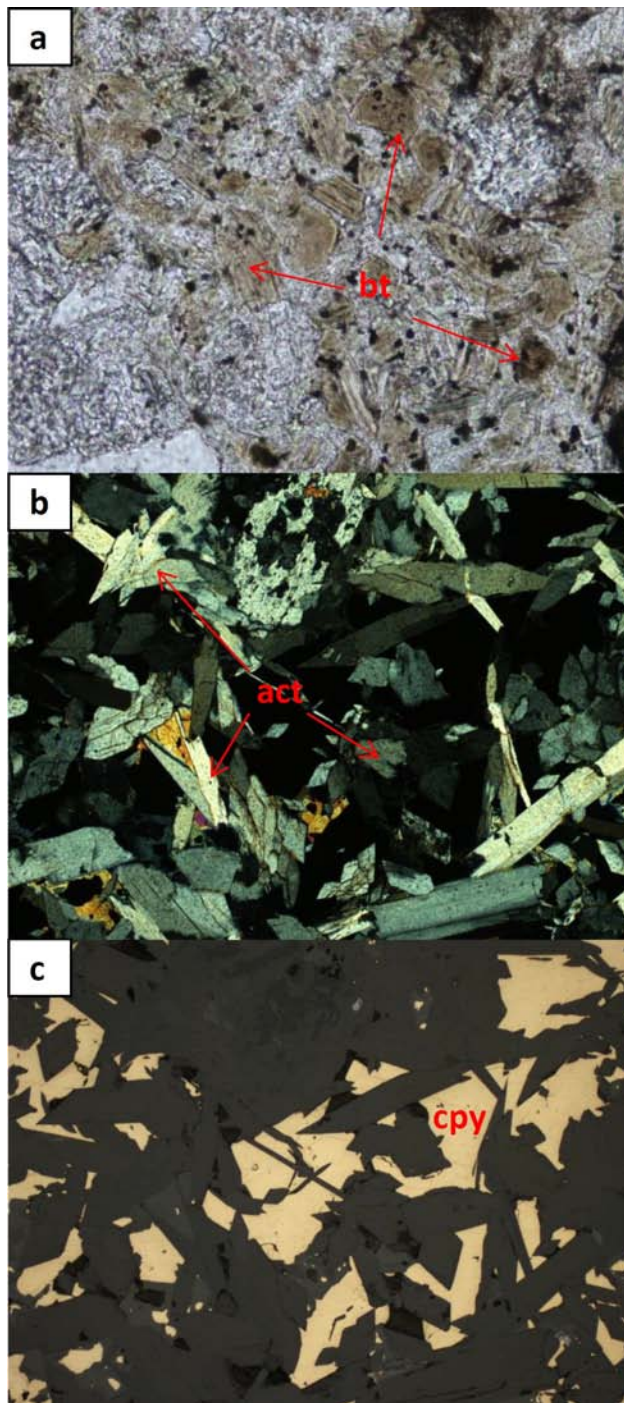


**Fig. 14.** Photomicrographs of mineralization at the Primer South from petrographic mounts cut from a hand sample like that shown in Figure 13c. **a)** Fine grained, brown booklets of secondary biotite partly altered to chlorite from sample MMI12-5-3, **b)** Cross polarized light view of sample MMI12-5-4 displays prisms and needles of euhedral actinolite intergrown with chalcopyrite (cpy) shown in reflected light in **c)**. Same field of view in all photos is 2 mm.

phyric volcanic strata show evidence of copper liberated during low grade regional metamorphism.

Copper-gold mineralization is associated with both potassic and calcic alteration of the dioritic intrusive

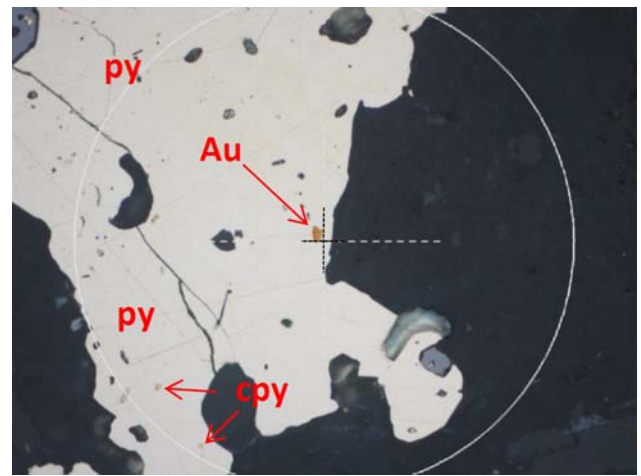


**Fig. 15.** Bright yellow-orange inclusion of gold (Au) in an irregular pyrite crystal (at crosshairs). Chalcopyrite (cpy) inclusions about half the size of the gold appear pale yellow in comparison, especially against the bright pyrite background (Sample MMI12-5-4, Primer South). Radius of the circle surrounding crosshair is 100 $\mu$ .

centres. Key mineral associations are K-feldspar-biotite-magnetite (and sulphides) and actinolite-epidote-calcite (and sulphides). Elevated gold values have been reported from mainly the eastern part of the property, although pyrite from the Primer South prospect, in the south-central part of the property, contains inclusions of gold (Fig. 16).

#### Acknowledgments

We thank T. Schroeter for pointing out the lack of base-line regional geological mapping information in the Dillard Creek area, and for sharing unpublished geochemical data (none included here). This paper was improved substantially by careful reviews by P. Schiarizza and L. Aspler.

#### References cited

- Church, B.N., 1973. Geology of the White Lake Basin. British Columbia Ministry of Energy, Mines and Petroleum Resources, British Columbia Geological Survey Bulletin 61, 141 p.
- Chapman, D.A., 1970. Geological reconnaissance report in Tectonic analysis of fracture density and geochemical report on the Dillard Creek property. British Columbia Ministry of Energy and Mines, British Columbia Geological Survey Assessment Report 2356, 8 p.
- Coney, P.J., Jones, D.L., and Monger, J.W.H., 1980. Cordilleran suspect terranes. *Nature*, 288, 329-333.
- Cormier, 1990. 1989 geochemical, geophysical and trenching report on the Dill claim: British Columbia Ministry of Energy, Mines and Petroleum Resources, British Columbia Geological Survey Assessment Report 19593, 21 p.
- Gutrath, G.C., 1980. Outcrop geology report, Prime claim group. British Columbia Ministry of Energy, Mines and Petroleum Resources, British Columbia Geological Survey Assessment Report 7521, 8 p.
- LeBas, M.J.L., Maitre, R.W.L., Streckeisen, A., and Zanettin, B., 1986. A chemical classification of volcanic rocks

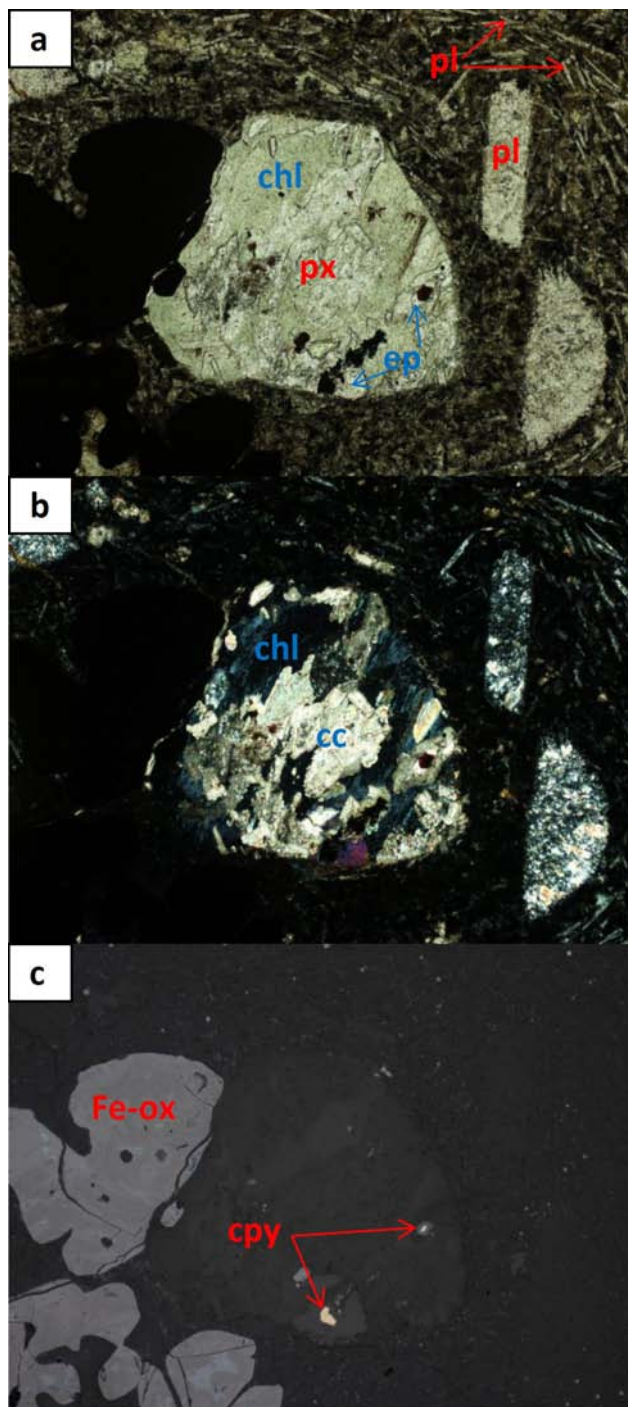


**Fig. 16.** Altered augite porphyry basalt in **a**) Plane polarized light displays a well-developed trachytic flow fabric (outlined by plagioclase microlites) that wraps around the pyroxene phenocrysts at the centre of the photo. Light green area is Fe-rich chlorite that displays anomalous blue interference colours in **b**) Cross polarized light. Much of the pyroxene is replaced by calcite (cc, high birefringence). Plagioclase phenocrysts are replaced by fine-grained? prehnite. **c**) In plane reflected light, bright yellow chalcopyrite is associated with epidote in altered pyroxene. Amoeboid grains on left are intergrowths of Fe-oxide and hydroxide minerals displaying an internal botryoidal fabric. Same field of view for all images; width is ~4 mm.

based on the total alkali-silica diagram. *Journal of Petrology* 27, 745-750.

- Logan, J.M. and Mihalynuk, M.G., 2005a. BC's 200 million year old porphyry Cu-Au deposits – an alkaline advantage, In: Association for Mineral Exploration British Columbia, Mineral Exploration Roundup, program with abstracts, pp. 13-15.
- Logan, J.M., and Mihalynuk, M.G., 2005b. Porphyry Cu-Au deposits of the Iron Mask Batholith, southeastern British Columbia. In: *Geological Fieldwork 2004*, British Columbia Ministry of Energy and Mines, British Columbia Geological Survey Paper 2005-1, pp. 271-290.
- Logan, J.M., and Mihalynuk, M.G., 2005c. Regional geology and setting of the Cariboo, Bell, Springer and Northeast Porphyry Cu-Au zones at Mount Polley, south-central, British Columbia. In: *Geological Fieldwork 2004*, British Columbia Ministry of Energy and Mines, British Columbia Geological Survey Paper 2005-1, pp. 249-270.
- Logan, J.M. and Mihalynuk, M.G., 2013a. Bonaparte gold: another 195 Ma Au-Cu porphyry deposit in southern British Columbia? In: *Geological Fieldwork 2012*, British Columbia Ministry of Energy, Mines and Natural Gas, British Columbia Geological Survey Paper 2013-1, (this volume).
- Logan, J.M., and Mihalynuk, M.G., 2013b. Tectonic controls on Early Mesozoic paired alkaline porphyry deposit belts (Cu-Au ± Ag-Pt-Pd-Mo) within the Canadian Cordillera. *Economic Geology*, in press.
- Logan, J.M., Mihalynuk, M.G., and Friedman, R.M., 2011. Age constraints of mineralization at the Brenda and Woodjam Cu-Mo+/-Au Porphyry deposits - An Early Jurassic calcalkaline event, south-central British Columbia. In: *Geological Fieldwork 2010*, British Columbia Ministry of Energy, Mines and Petroleum Resources, British Columbia Geological Survey Paper 2011-1, pp. 129-144.
- Massey, N.W.D., MacIntyre, D.G., Desjardins, P.J., and Cooney, R.T., 2005. Digital Geology Map of British Columbia. British Columbia Ministry of Energy, Mines and Petroleum Resources, British Columbia Geological Survey Open File 2005-1; URL accessed November, 2012, <http://www.empr.gov.bc.ca/Mining/Geoscience/PublicationsCatalogue/GeoFiles/Pages/2005-1.aspx>.
- Mihalynuk, M.G., 2010. Recipe for Cu-Au-Ag ±Mo porphyry deposits: Ingredients from the northern Cordilleran terranes. In: *Copper Porphyry Workshop*, Geological Association of Canada, Vancouver, BC, Canada.
- Mihalynuk, M.G., and Logan, J.M., 2013a. Geological setting of Late Triassic Cu-Au porphyry mineralization at Miner Mountain, Princeton. In: *Geological Fieldwork 2012*, British Columbia Ministry of Energy, Mines and Natural Gas, British Columbia Geological Survey Paper 2013-1, (this volume).
- Mihalynuk, M.G., Logan, J.M., 2013b. Lithogeochemical data from porphyry environments between Princeton and Merritt, BC Ministry of Energy, Mines and Natural Gas, Geofile 2013, in press.
- Mihalynuk, M.G., Logan, J.M., Friedman, R.M., and Preto, V.A., 2010. Age of mineralization and “Mine Dykes” at Copper Mountain alkaline copper-gold-silver porphyry deposit (NTS 092H/07), South-Central British Columbia. In: *Geological Fieldwork 2009*, BC Ministry of Energy, Mines and Petroleum Resources Paper 2010-1, pp. 163-171.

- Monger, J.W.H., 1989. Geology, Hope, British Columbia. Geological Survey of Canada, Map 41-1989, scale 1:250 000.
- Parrish, R.R., and Monger, J.W.H., 1992. New U-Pb dates from southwestern British Columbia. In: Geological Survey of Canada, Radiogenic age and isotopic studies; Report 5, 87-108.
- Pearce, J.A., 1996. A user's guide to basalt discrimination diagrams. Short Course Notes - Geological Association of Canada 12, pp. 79-113.
- Peccerillo, A., Taylor, S.R., 1976. Rare earth elements in the East Carpathian volcanic rocks. *Earth and Planetary Science Letters*, 32, 121-126.
- Preto, V.A., 1979. Geology of the Nicola Group between Merritt and Princeton. British Columbia Ministry of Energy, Mines and Petroleum Resources, British Columbia Geological Survey Bulletin 69, 90 p.
- Pringle, D., 1969. Tectonic analysis of fracture density and geochemical report on the Dillard Creek property. British Columbia Ministry of Energy and Mines, British Columbia Geological Survey Assessment Report 2356, 91 p.
- Rice, H.M.A., 1947. Geology and mineral deposits of the Princeton map-area, British Columbia Geological Survey of Canada, Memoir 243, 136 p.
- Sun, S.S., McDonough, W.F., 1989. Chemical and isotopic systematics of oceanic basalts; implications for mantle composition and processes. *Geological Society Special Publication* 42, pp. 313-345.
- Tipper, H.W., Woodsworth, G.J., and Gabrielse, H., 1981. Tectonic assemblage map of the Canadian Cordillera and adjacent parts of the United States of America. Geological Survey of Canada, Map 1712A, scale 1:2 000 000.
- Tully, D., 1970 Report on diamond drill and geochemical results on Dillard Creek property. British Columbia Ministry of Energy and Mines, British Columbia Geological Survey Assessment Report 2354, 108 p.

